SUPPORTING INFORMATION FOR

Accelerating the Coupling of Maleated Polyolefins with Polyesters

via Tin Compounds

Nathan P. Birch, Kunwei Liu, Sung Cik Mun, Gagik Ghazaryan, Claire T. Senger, Christopher J. Ellison*, Christopher W. Macosko*

Department of Chemical Engineering and Materials Science, University of Minnesota, Minneapolis, Minnesota 55414-0431, United States

Christopher M. Thurber, Thomas H. Peterson, Sukrit Mukhopadhyay

The Dow Chemical Co., Midland, Michigan 48674

Corresponding Authors: * cellison@umn.edu; phone (612) 626-9834. *macosko@umn.edu; phone (612) 625-0092 (C.W.M.).

Materials

Polyethylene terephthalate glycol (PETG, Skygreen® K2012) was obtained from SK Chemical. Linear low density maleated polyethylene (LLDPE-MAH, 0.25% MAH, MI 1.0, density 0.922 g/cm^3) was obtained from Dow Chemical Co.

Degradation of polyethylene terephthalates at long mixing times

A reduction in force at long mixing times was observed during microcompounding. Given the high temperatures and use of metal additives a reduction in the molecular weight of PET was suspected.[1] Mixing data for pure PET and PETG with DOTO additive were obtained below, showing degradation at 270°C. It is notable that thermal degradation rate in the presence of divalent metal additives is higher in PET than PETG as the terephthalic acid-ethylene glycol linkages degrade and the terephthalic acid-cyclohexane dimethanol linkages do not. PETG at 220°C did not significantly degrade.
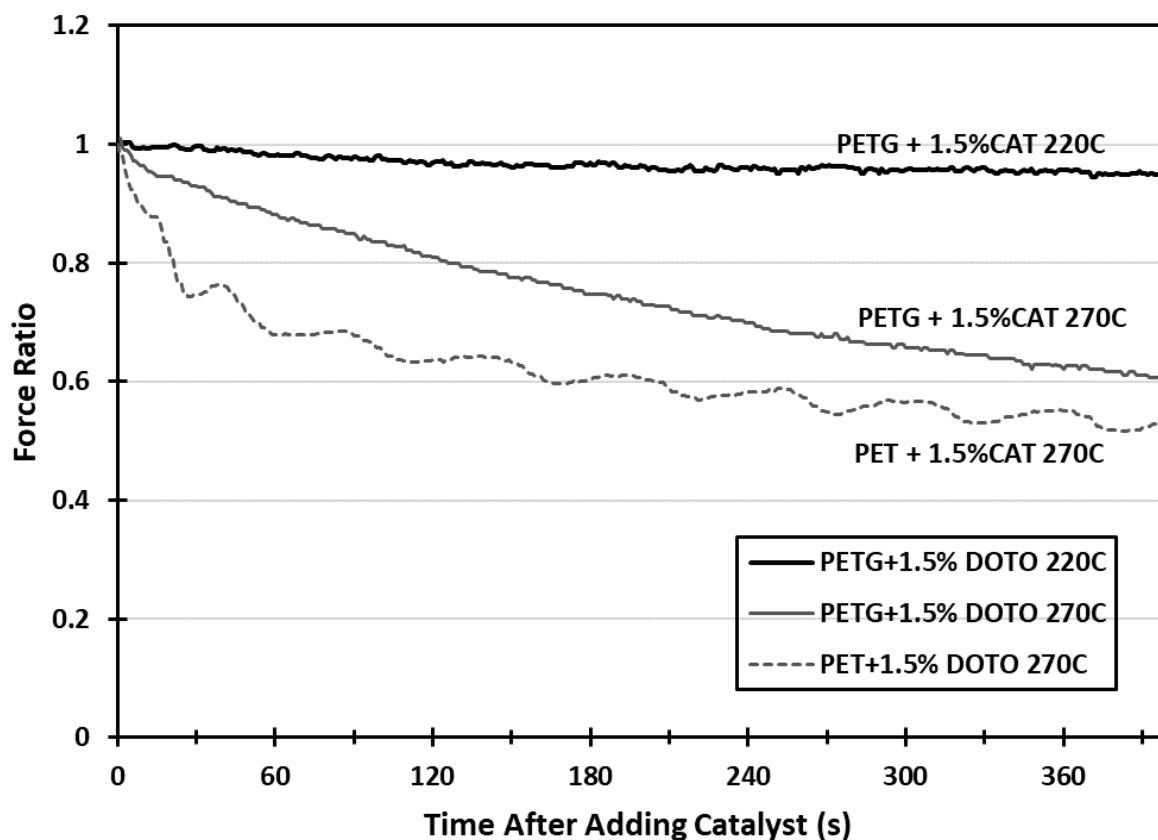

Figure S1: PET microcompounded with 1.5% w/w DOTO at 220°C and 270°C, rapid thermal degradation results in decreasing force ratio.

Crosslinking of maleated polyethylenes during compounding

During compounding of PE-MAH and DOTO in a Haake™ Rheomix OS labmixer (Thermo Fisher Scientific, RheoDrive 4, Rheomix 600, roller rotors) at 160°C, significant crosslinking was observed. Rheology on the resultant blend (below) indicated a much higher G' at low frequencies, supporting the presence of crosslinks. Follow up experiments were able to demonstrate that crosslinking did not occur the absence of oxygen. Both wet and dry nitrogen were explored to demonstrate that environmental oxygen was the culprit rather than environmental water. HDPE-MAH crosslinking has previously been reported to be exacerbated by the presence of atmospheric oxygen and DOTO maybe catalyzing this undesirable reaction.[2]
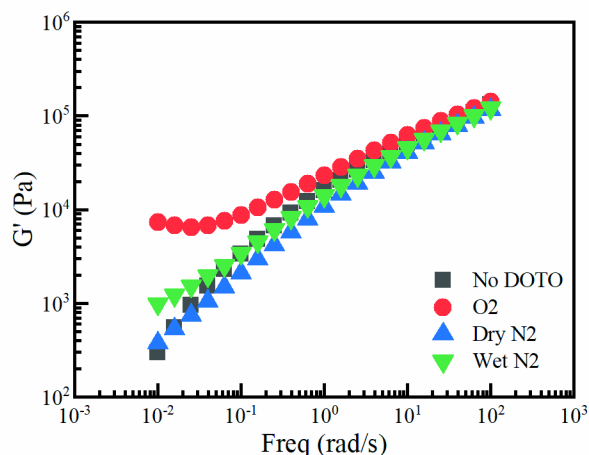

Figure S2: Rheology of PE-MAH after microcompounding with DOTO at 160°C without DOTO (■), in the presence of atmospheric oxygen (●), in a dry nitrogen bath (▲), in a wet nitrogen bath (▼).

SEM Imaging

Laminated bilayers were cryo-microtomed at -140 °C in a Leica EM UC6 microtome using a diamond knife. The cross-sectional surfaces were then coated with ~2 nm of iridium using an ACE600 coater. For each interface, about 10 SEM micrographs were taken with a Hitachi S-4700 microscope.
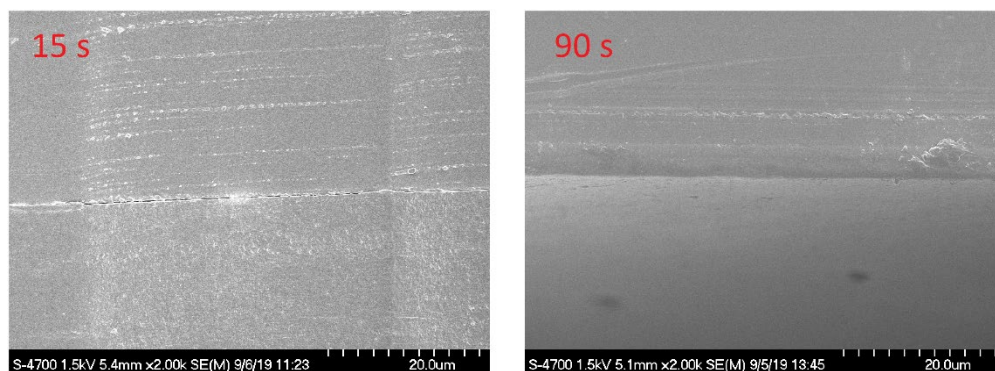
Figure S3: SEM images of HDPE-MAH (1%) containing 0.8% DOTO and PET bilayers laminated for 15 s and 90 s contact time.

Synthesis of di-n-octyltin succinate and ^{1}H NMR spectra

Dibutyltin maleate is easily formed from dibutyltin oxide and maleic anhydride through heated mixing.[3] The low temperatures involved suggest a relatively favorable reaction. In order to prove that di-n-octyltin oxide and succinic anhydride react in a similar way and gather background information for expected NMR spectra in the model system, di-n-octyltin succinate was synthesized. 6g of di-n-octlytin oxide and 1.68g of succinic anhydride were placed in a round bottom flask. 60 mL of benzene was added to the flask and brought to gentle reflux. After 2 hours, the resultant mixture was subjected to vacuum in a rotary evaporator at 25°C until all benzene has been driven off. The resultant powder was suspended in acetone and vacuum filtered over fine fritted glass. The filtride was then dried under vacuum at room temperature overnight. NMR spectra were obtained by dissolving the product in deuterated chloroform and measuring the resultant mixture in a 400 MHz Bruker NMR spectrometer (RT, CDCl$_3$, n=16, d1=1s). The resultant spectra (Figure S4) show a clear shift in the succinate peak from 3.0 to 2.64.
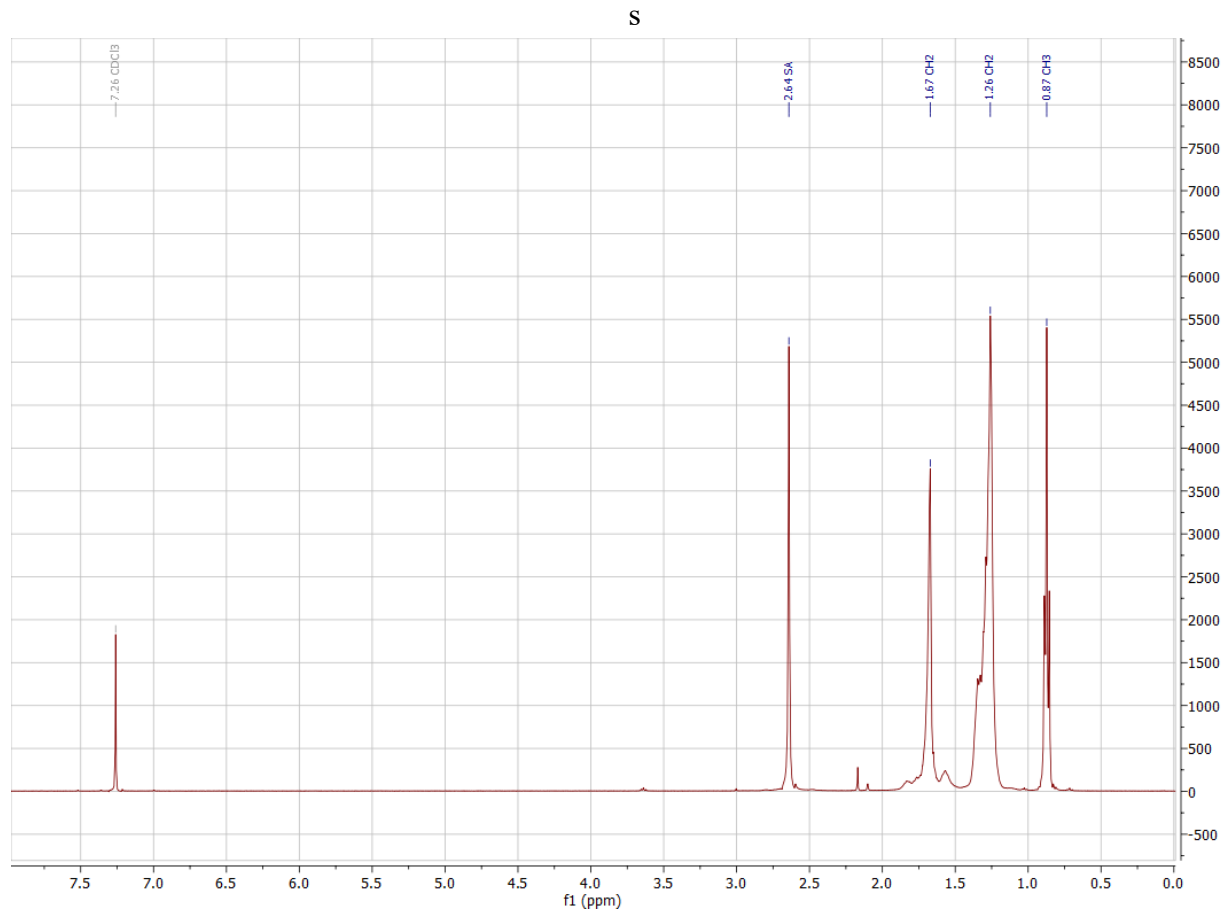
S

Figure S4: 1H-NMR of di-n-octyltin succinate in CDCl₃. 0.87 peak is terminal CH₃ groups, 1.67 and 1.26 peaks are CH₂ groups, and 2.64 is the shifted succinate peak. Unshifted succinate peak (no reaction) was previously found at 3.00.

Sample ¹H-NMR spectra of reaction products

As discussed in the paper body, the relative size of the integrals from 4.2-4.0 and 3.85-3.45 (Figure S5) were used to determine the relative concentrations of unreacted hexadecanol and reacted hexadecanol-OSA product.
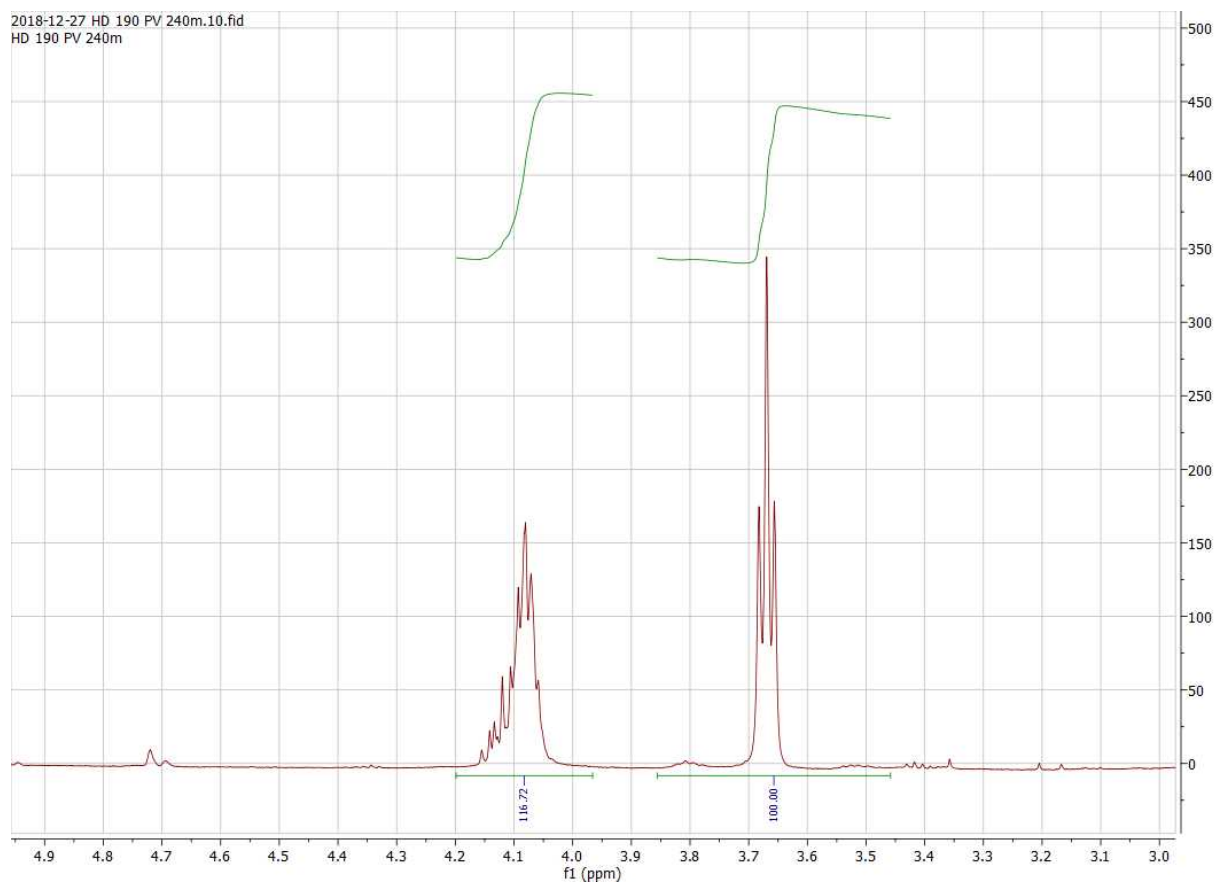
Figure S5: Region of interest from ^{1}H-NMR spectra of product mixture for 200 mM HD, 100 mM OSA, 100 mM DOTO at 190°C, 240 min aliquot. Peaks from 4.2-4.0 are from reacted hexadecanol. Peaks from 3.85-3.45 are from unreacted hexadecanol.

As discussed in the paper body, the relative size of the integrals from 8.13-8.11, 8.08-8.06, 8.05-8.04 (Figure S6) were used to determine the relative concentrations of interesterification product, EGB, and the side product.
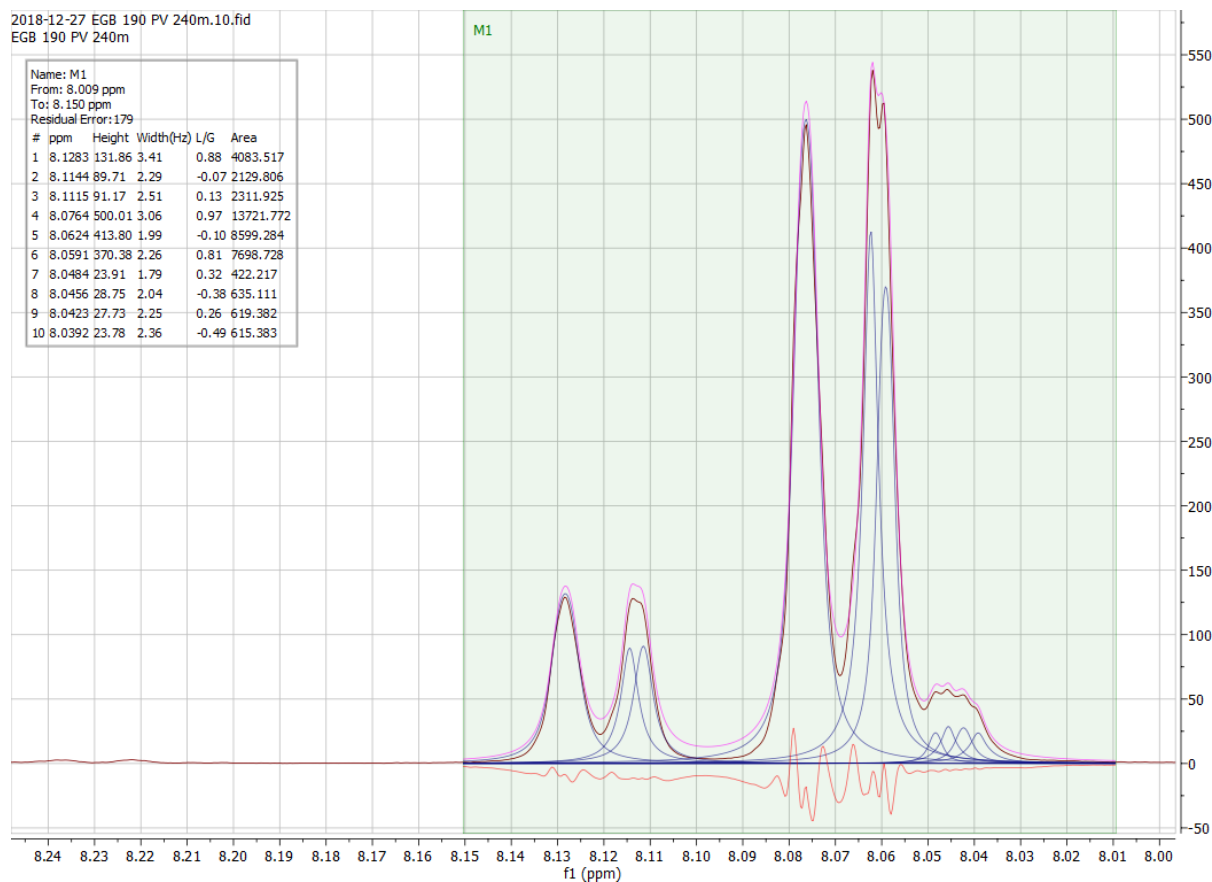
Figure S6: Region of interest of ^{1}H-NMR spectra of product mixture for 100 mM EGB, 100 mM OSA, 100 mM DOTO at 190°C, 240 min aliquot. Product peaks are 8.13-8.11, EGB 8.08-8.06, and a side product has peaks 8.05-8.04.

Computational Evaluation of the Interesterification Mechanism

The structures of hypothesized species in ground and transition states were optimized using Density Functional Theory (DFT) at B3LYP/6-31g* level.[4–9] For Sn, LANL2DZ basis set is used. The effect of dispersion is included using the D3 version of Grimme's dispersion with Becke-Johnson damping.[10] For simplicity, the octyl chains are replaced by methyl groups in di-n-octyltin octyl succinate. After obtaining the optimized geometries, the energies of each species are computed using the same DFT functional and LANL2DZ basis for Sn and larger basis set (6-311+g**)[4–9] for other atoms. The vibrational analysis on the ground state geometries was performed and the lack of imaginary frequencies was used to ascertain the minima on the potential energy surface (PES). On the other hand, the same analysis on the transition state geometries indicated one imaginary frequency. In the latter case, the GaussView program was used to visualize the vibrational mode with imaginary frequency in order to ensure that the atoms moved along the desired reaction coordinate. For both ground state and transition state, various conformations were explored and the energies of the lowest conformation were used to calculate

thermodynamic properties and barrier heights. These calculations were performed using G09 suit of programs.[11]

Figure S7A depicts the reaction between model compounds. At first, the dibenzoate binds with tin succinate, whose binding energy is denoted as ΔE_{Bind}. Once the ester binds with the tin succinate, interesterification occurs, whose barrier height is denoted as ΔE_{TS}. The thermodynamics of the overall reaction are denoted as ΔE_{Rxn}. Figure S7B depicts the structures of the model tin succinate, the transition state for interesterification and the final product. Table S1 lists the computed energetics. The interesterification process is thermodynamically favored because the Sn atom assumes octahedral geometry by coordinating with the carbonyl groups of the ester moieties. In addition, there is also a possibility of intramolecular π-stacking between the phenyl groups, which is not possible in the reactant. The computed barrier height for the interesterification process is found to be 97.9 kJ/mol, which is comparable with experimental findings. Therefore, interesterification seems to be a viable route for PET grafted PE.
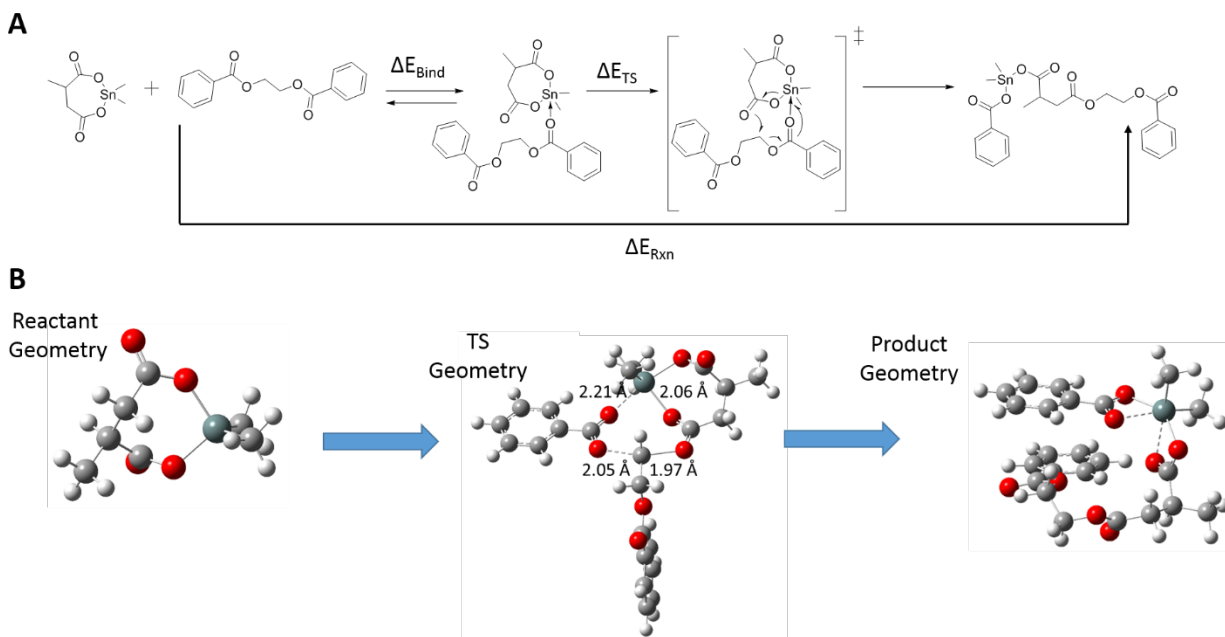

Figure S7: (A) Interesterification reaction between model tin succinate and ethylene glycol dibenzoate; (B) computed geometries of reactant, transition state and product.

Table S1: Computed energetics (ΔE_{Bind}, ΔE_{TS} and ΔE_{Rxn}) for the interesterification reaction; the nomenclature is depicted in Figure S6A

ΔE_{Bind} (kJ/mol)	ΔE_{TS} (kJ/mol)	ΔE_{Rxn} (kJ/mol)
-55.6	97.9	-148.5

References

(1)   Zimmerman, H.; Kim, N. T. Investigations on Thermal and Hydrolytic Degradation of Poly(Ethylene Terephthalate). *Polym. Eng. Sci.* **1980**, *20* (10), 680–683. https://doi.org/10.1002/pen.760201008.

(2)   Ghaemy, M.; Roohina, S. Grafting of Maleic Anhydride on Polyethylene in a Homogeneous Medium in the Presence of Radical Initiators. *Iran. Polym. J.* **2002**, *12* (1), 21–29.

(3)   Hirshman, J. L.; Breza, E. J. Process for Preparing Dibutyltin Maleate. 3522282, 1970.

(4)   Becke, A. D. Density-functional Thermochemistry. III. The Role of Exact Exchange. *J. Chem. Phys.* **1993**, *98* (7), 5648–5652. https://doi.org/10.1063/1.464913.

(5)   Lee, C.; Yang, W.; Parr, R. G. Development of the Colle-Salvetti Correlation-Energy Formula into a Functional of the Electron Density. *Phys. Rev. B* **1988**, *37* (2), 785–789. https://doi.org/10.1103/PhysRevB.37.785.

(6)   Miehlich, B.; Savin, A.; Stoll, H.; Preuss, H. Results Obtained with the Correlation Energy Density Functionals of Becke and Lee, Yang and Parr. *Chem. Phys. Lett.* **1989**, *157* (3), 200–206. https://doi.org/10.1016/0009-2614(89)87234-3.

(7)   Ditchfield, R.; Hehre, W. J.; Pople, J. A. Self-Consistent Molecular-Orbital Methods. IX. An Extended Gaussian-Type Basis for Molecular-Orbital Studies of Organic Molecules. *J. Chem. Phys.* **1971**, *54* (2), 724–728. https://doi.org/10.1063/1.1674902.

(8)   Hehre, W. J.; Ditchfield, R.; Pople, J. A. Self—Consistent Molecular Orbital Methods. XII. Further Extensions of Gaussian—Type Basis Sets for Use in Molecular Orbital Studies of Organic Molecules. *J. Chem. Phys.* **1972**, *56* (5), 2257–2261. https://doi.org/10.1063/1.1677527.

(9)   Gordon, M. S. The Isomers of Silacyclopropane. *Chem. Phys. Lett.* **1980**, *76* (1), 163–168. https://doi.org/10.1016/0009-2614(80)80628-2.

(10)   Grimme, S.; Ehrlich, S.; Goerigk, L. Effect of the Damping Function in Dispersion Corrected Density Functional Theory. *J. Comput. Chem.* **2011**, *32* (7), 1456–1465. https://doi.org/10.1002/jcc.21759.

(11)   Frisch, M. J.; Trucks, G. W.; Schlegel, H. B.; Scuseria, G. E.; Robb, M. A.; Cheeseman, J. R.; Scalmani, G.; Barone, V.; Petersson, G. A.; Nakatsuji, H.; et al. Guassian 09, Revision A.02. Gaussian, Inc: Wallingford CT 2016.